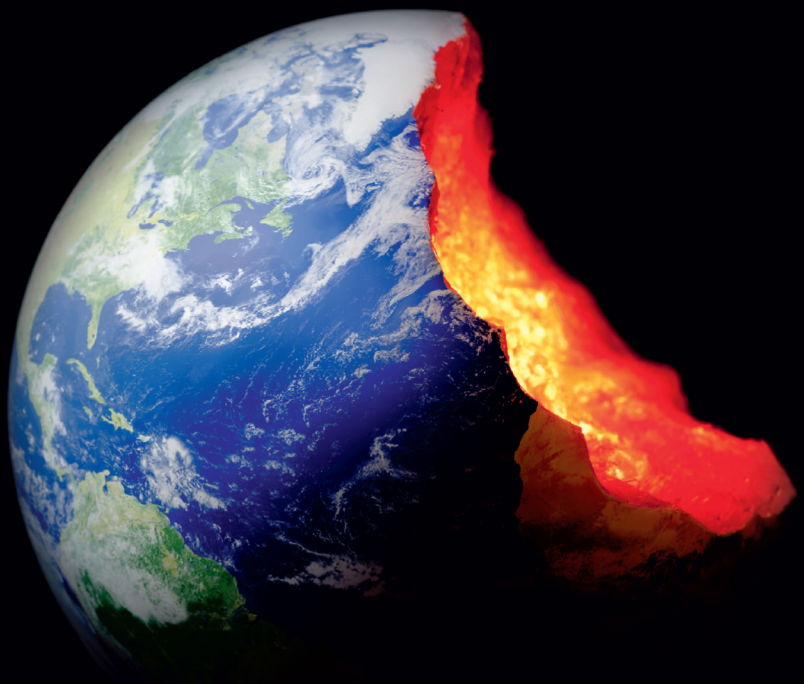

Physics and Chemistry of the Deep Earth

Edited by **Shun-ichiro Karato**

WILEY-BLACKWELL

PHYSICS AND CHEMISTRY OF THE DEEP EARTH

Physics and Chemistry of the Deep Earth

Edited by

Shun-ichiro Karato
Department of Geology and Geophysics
Yale University, New Haven
CT, USA

WILEY-BLACKWELL
A John Wiley & Sons, Ltd., Publication

This edition first published 2013 © 2013 by John Wiley & Sons, Ltd.

Wiley-Blackwell is an imprint of John Wiley & Sons, formed by the merger of Wiley's global Scientific, Technical and Medical business with Blackwell Publishing.

Registered office: John Wiley & Sons, Ltd, The Atrium, Southern Gate, Chichester, West Sussex, PO19 8SQ, UK

Editorial offices: 9600 Garsington Road, Oxford, OX4 2DQ, UK
The Atrium, Southern Gate, Chichester, West Sussex, PO19 8SQ, UK
111 River Street, Hoboken, NJ 07030-5774, USA

For details of our global editorial offices, for customer services and for information about how to apply for permission to reuse the copyright material in this book please see our website at www.wiley.com/wiley-blackwell.

Library of Congress Cataloging-in-Publication Data

Physics and chemistry of the deep Earth / Shun-ichiro Karato.
pages cm
Includes bibliographical references and index.
ISBN 978-0-470-65914-4 (cloth)
1. Geophysics. 2. Geochemistry. 3. Earth – Core. I. Karato, Shun-ichiro, 1949-
QE501.K325 2013
551.1′2 – dc23

2012045123

A catalogue record for this book is available from the British Library.

Wiley also publishes its books in a variety of electronic formats. Some content that appears in print may not be available in electronic books.

Cover image: © iStockphoto.com/Thomas Vogel
Cover design by Design Deluxe

Set in 9/11.5pt Trump Mediaeval by Laserwords Private Limited, Chennai, India

1 2013

Contents

Colour plate section can be found between pages 214–215

Contributors

JENNIFER ANDREWS *Bullard Laboratory, Cambridge University, Cambridge, UK*

ELIZABETH DAY *Bullard Laboratory, Cambridge University, Cambridge, UK*

ARWEN DEUSS *Bullard Laboratory, Cambridge University, Cambridge, UK*

ANDREAS FICHTNER *Department of Earth Sciences, Utrecht University, Utrecht, The Netherland*

HIKARU IWAMORI *Department of Earth and Planetary Sciences, Tokyo Institute of Technology, Tokyo, Japan*

SHUN-ICHIRO KARATO *Department of Geology and Geophysics, Yale University, New Haven, CT, USA*

KENJI KAWAI *Department of Earth and Planetary Sciences, Tokyo Institute of Technology, Tokyo, Japan*

HANS KEPPLER *Byerisched Geoinstitut, Universität Bayreuth, Bayreuth, Germany*

KONSTANTIN LITASOV *Department of Earth and Planetary Materials Science, Graduate School of Science, Tohoku University, Sendai, Japan*

MOTOHIKO MURAKAMI *Department of Earth and Planetary Materials Science, Graduate School of Science, Tohoku University, Sendai, Japan*

TOMOEKI NAKAKUKI *Department of Earth and Planetary Systems Science, Hiroshima University, Hiroshima, Japan*

EIJI OHTANI *Department of Earth and Planetary Materials Science, Graduate School of Science, Tohoku University, Sendai, Japan*

ANTON SHATSKIY *Department of Earth and Planetary Materials Science, Graduate School of Science, Tohoku University, Sendai, Japan*

YASUKO TAKEI *Earthquake Research Institute, University of Tokyo, Tokyo, Japan*

JEANNOT TRAMPERT *Department of Earth Sciences, Utrecht University, Utrecht, The Netherland*

TAKU TSUCHIYA *Geodynamic Research Center, Ehime University, Matsuyama, Ehime, Japan*

DIANA VALENCIA *Department of Earth, Atmospheric and Planetary Sciences, Massachusetts Institute of Technology, Cambridge, MA, USA*

PETER VAN KEKEN *Department of Earth and Environmental Sciences, University of Michigan, Ann Arbor, MI, USA*

DUOJUN WANG *Graduate University of Chinese Academy of Sciences, College of Earth Sciences, Beijing, China*

Preface

Earth's deep interior is largely inaccessible. The deepest hole that human beings have drilled is only to ~11 km (Kola peninsula in Russia) which is less than 0.2 % of the radius of Earth. Some volcanoes carry rock samples from the deep interior, but a majority of these rocks come from less than ~200 km depth. Although some fragments of deep rocks (deeper than 300 km) are discovered, the total amount of these rocks is much less than the lunar samples collected during the Apollo mission. Most of geological activities that we daily face occur in the shallow portions of Earth. Devastating earthquakes occur in the crust or in the shallow upper mantle (less than ~50 km depth), and the surface lithosphere (''plates'') whose relative motion controls most of near surface geological activities has less than ~100 km thickness. So why do we worry about ''deep Earth''?

In a sense, the importance of deep processes to understand the surface processes controlled by plate tectonics is obvious. Although plate motion appears to be nearly two-dimensional, the geometry of plate motion is in fact three-dimensional: Plates are created at mid-ocean ridges and they sink into the deep mantle at ocean trenches, sometimes to the bottom of the mantle. Plate motion that we see on the surface is part of the three-dimensional material circulation in the deep mantle. High-resolution seismological studies show evidence of intense interaction between sinking plates and the deep mantle, particularly the mid-mantle (transition zone) where minerals undergo a series of phase transformations. Circulating materials of the mantle sometimes go to the bottom (the core–mantle boundary) where chemical interaction between these two distinct materials occurs. Deep material circulation is associated with a range of chemical processes including partial melting and dehydration and/or rehydration. These processes define the chemical compositions of various regions, and the material circulation modifies the materials' properties, which in turn control the processes of materials circulation.

In order to understand deep Earth, a multidisciplinary approach is essential. First, we need to know the behavior of materials under the extreme conditions of deep Earth (and of deep interior of other planets). Drastic changes in properties of materials occur under the deep planetary conditions including phase transformations (changes in crystal structures and melting). Resistance to plastic flow also changes with pressure and temperature as well as with water content. Secondly, we must develop methods to infer deep Earth structures from the surface observations. Thirdly, given some observations, we need to develop a model (or models) to interpret them in the framework of physical/chemical models.

In this book, a collection of papers covering these three areas is presented. The book is divided into three parts. The first part (Keppler, Litasov *et al.*, Takei, Karato, Karato and Wang) includes papers on materials properties that form the basis

for developing models and interpreting geophysical/geochemical observations. The second part (Murakami, Tsuchiya and Kawai, Ohtani, Valencia) contains papers on the composition of deep Earth and planets including the models of the mantle and core of Earth as well as models of super-Earths (Earth-like planets orbiting stars other than the Sun). And finally the third part (Deuss *et al*., Trampert and Fichtner, van Keken, Iwamori) provides several papers that summarize seismological and geochemical observations pertinent to deep mantle materials circulation and geodynamic models of materials circulation where geophysical/geochemical observations and mineral physics data are integrated. All of these papers contain reviews of the related area to help readers understand the current status of these areas.

I thank all the authors and reviewers and editors of Wiley-Blackwell who made it possible to prepare this volume. I hope that this volume will help readers to develop their own understanding of this exciting area of research and to play a role in the future of deep Earth and planet studies.

Shun-ichiro Karato
New Haven, Connecticut

Part 1

Materials' Properties

1 Volatiles under High Pressure

HANS KEPPLER

Bayerisches Geoinstitut, Universität Bayreuth, Bayreuth, Germany

Summary

Hydrogen and carbon are the two most important volatile elements in the Earth's interior, yet their behavior is very different. Hydrogen is soluble in mantle minerals as OH point defects and these minerals constitute a water reservoir comparable in size to the oceans. The distribution of water in the Earth's interior is primarily controlled by the partitioning between minerals, melts and fluids. Most of the water is probably concentrated in the minerals wadsleyite and ringwoodite in the transition zone of the mantle. Carbon, on the other hand, is nearly completely insoluble in the silicates of the mantle and therefore forms a separate phase. Stable carbon-bearing phases are likely carbonates in the upper mantle and diamond or carbides in the deeper mantle. Already minute amounts of water and carbon in its oxidized form (as carbonate or CO_2) greatly reduce the solidus of mantle peridotite. Melting in subduction zones is triggered by water and both water and CO_2 contribute to the melting below mid-ocean ridges and in the seismic low-velocity zone. Redox melting may occur when oxygen fugacity increases upon upwelling of reduced deep mantle, converting reduced carbon species to carbonate or CO_2 that strongly depress solidus temperatures. The large contrast of water storage capacity between transition zone minerals and the mineral assemblages of the upper and lower mantle implies that melt may form near the 440 and 660 km seismic discontinuities. Water and carbon have been exchanged during the Earth's history between the surface and the mantle with typical mantle residence times in the order of billions of years. However, the initial distribution of volatiles between these reservoirs at the beginning of the Earth's history is not well known. Nitrogen, noble gases, sulfur and halogens are also continuously exchanged between mantle, oceans and atmosphere, but the details of these element fluxes are not well constrained.

1.1 Introduction: What Are Volatiles and Why Are They Important?

Volatiles are chemical elements and compounds that tend to enter the gas phase in high-temperature magmatic and metamorphic processes. Accordingly, one can get some idea about the types of volatiles occurring in the Earth's interior by looking at compositions of volcanic gases. Table 1.1 compiles some typical volcanic gas analyses. As is obvious from this table, water and carbon dioxide are the two most abundant volatiles and they are also most important for the dynamics of the Earth's interior (e.g. Bercovici & Karato, 2003; Mierdel *et al.*, 2007; Dasgupta & Hirschmann, 2010). Other, less abundant volatiles are sulfur and halogen

Physics and Chemistry of the Deep Earth, First Edition. Edited by Shun-ichiro Karato.

Table 1.1 Composition of volcanic gases (in mol%).

	Mt. St. Helens 1980	Kilauea 1918	Kilauea 1983	Etna 2000
H_2O	91.6	37.1	79.8	92
H_2	0.85	0.49	0.90	
CO_2	6.94	48.9	3.15	7.3
CO	0.06	1.51	0.06	
SO_2	0.21	11.84	14.9	1.0
H_2S	0.35	0.04	0.62	
HCl		0.08	0.1	0.1
HF			0.19	0.07

Source: Data from Symonds *et al*. (1994) except for Etna (from Allard *et al*., 2005).

compounds, particularly SO_2, H_2S, HCl, and HF. Noble gases are only trace constituents of volcanic gases, but they carry important information on the origins and history of the reservoirs they are coming from (Graham, 2002; Hilton *et al*., 2002). Nitrogen is a particular case. Volcanic gas analyses sometimes include nitrogen, but it is often very difficult to distinguish primary nitrogen from contamination by air during the sampling process. The most conclusive evidence for the importance of nitrogen as a volatile component in the Earth's interior is the occurrence of N_2-filled fluid inclusions in eclogites and granulites (Andersen *et al*., 1993). Ammonium (NH_4^+) appears to be a common constituent in metamorphic micas, which may therefore recycle nitrogen into the mantle in subduction zones (Sadofsky & Bebout, 2000).

Generally, the composition of fluids trapped as fluid inclusions in magmatic and metamorphic rocks of the Earth's crust is similar to volcanic gases. Water and carbon dioxide prevail; hydrous fluid inclusions often contain abundant dissolved salts. Methane (CH_4) containing inclusions are also sometimes found, particularly in low-grade metamorphic rocks of sedimentary origin and in sediments containing organic matter (Roedder, 1984). Fluid inclusions in diamonds are an important window to fluid compositions in the mantle. Observed types include CO_2-rich inclusions, carbonatitic compositions, water-rich inclusions with often very high silicate content, and highly saline brines (Navon *et al*., 1988; Schrauder & Navon, 1994; Izraeli *et al*., 2001). Methane and hydrocarbon-bearing inclusions have also been reported from xenoliths in kimberlites (Tomilenko *et al*., 2009).

Although volatiles are only minor or trace constituents of the Earth's interior, they control many aspects of the evolution of our planet. This is for several reasons: (1) Volatiles, particularly water and carbon dioxide, strongly reduce melting temperatures; melting in subduction zones, in the seismic low velocity zone and in deeper parts of the mantle cannot be understood without considering the effect of water and carbon dioxide (e.g. Tuttle & Bowen, 1958; Kushiro, 1969; Kushiro, 1972; Tatsumi, 1989; Mierdel *et al*., 2007; Hirschmann, 2010). (2) Even trace amount of water dissolved in major mantle minerals such as olivine can reduce their mechanical strength and therefore the viscosity of the mantle by orders of magnitude (Mackwell *et al*., 1985; Karato & Jung, 1998; Kohlstedt, 2006). Mantle convection and all associated phenomena, such as plate movements on the Earth's surface, are therefore intimately linked to the storage of water in the mantle. (3) Hydrous fluids and carbonatite melts only occur in trace amounts in the Earth's interior. Nevertheless they are responsible for chemical transport processes on local and on global scales (e.g. Tatsumi, 1989; Iwamori *et al*., 2010). (4) The formation and evolution of the oceans and of the atmosphere is directly linked to the outgassing of the mantle and to the recycling (''ingassing'') of volatiles into the mantle (e.g. McGovern & Schubert, 1989; Rüpke *et al*., 2006; Karato, 2011).

1.2 Earth's Volatile Budget

The Earth very likely formed by accretion of chondritic material that resembles the bulk composition of the solar system. In principle, it should therefore be possible to estimate the Earth's volatile budget by considering the volatile content of chondritic meteorites (e.g. Morbidelli

et al., 2002; Albarède, 2009). Unfortunately, there is a large variation in the contents of water, carbon and other volatiles between the different kinds of chondritic meteorites and the Earth, likely formed by accretion of a mixture of these different materials, the precise fractions being poorly constrained. Moreover, during accretion, massive loss of volatiles to space likely occurred caused by impacts. This volatile loss has to be accounted for, which introduces another, considerable uncertainty.

Estimating the volatile content of the bulk mantle or of the bulk silicate Earth (crust + mantle) from cosmochemical arguments is even more difficult, since the iron–nickel alloy of the Earth's core very likely sequestered at least some fraction of the available volatiles. Evidence for this comes from the occurrence of sulfides (troilite, FeS), carbides (cohenite, Fe_3C) and nitrides (osbornite, TiN) as minerals in iron meteorites and from various experimental studies that show that under appropriate conditions, carbon, sulfur, nitrogen and hydrogen are quite soluble in molten iron (Fukai, 1984; Wood, 1993; Okuchi, 1997; Adler & Williams, 2005; Terasaki *et al.*, 2011). Another line of evidence is the density deficit of the Earth's outer core (Birch, 1952), which requires the presence of some light elements in the iron nickel melt. While most present models suggest that Si and/or O account for most of the density deficit, a significant contribution from other volatiles is possible. The recent model by Rubie *et al.* (2011) yields 8 wt % Si, 2 wt % S and 0.5 wt % O as light elements in the core. The low oxygen content appears to be consistent with shock wave data on melts in the Fe–S–O system (Huang *et al.*, 2011).

The timing of volatile acquisition on the Earth is another poorly constrained variable. One type of models assumes that volatiles were acquired during the main phase of accretion, while another view holds that volatiles, in particular water were delivered to the Earth very late (Albarède, 2009), possibly during the formation of a ''late veneer'' of chondritic materials or perhaps by comets. However, both the D/H and $^{15}N/^{14}N$ isotope ratios of terrestrial reservoirs are close to the chondritic values, while they are much lower than those observed in comets. This limits the cometary contribution to the terrestrial water and nitrogen budget to a few percent at most (Marty & Yokochi, 2006).

Recent models of the Earth's formation (e.g. Rubie *et al.*, 2011) suggest that during accretion, initially very volatile depleted chondritic material accreted, which possibly became more water and volatile-rich towards the end of accretion, but still before core formation. Such models are consistent with the observed depletion of moderately volatile elements (e.g. Na, K, Zn) on the Earth relative to CI chondrites; these elements may have failed to condense in chondritic material that formed close to the sun. Numerical models of early solar system evolution suggest that at later stages of accretion, stronger radial mixing in the solar system occurred, so that water and volatile-rich material from the cold outer part of the solar system entered the growing planet (Morbidelli *et al.*, 2002). Taking all of the available evidence together, it is plausible that the Earth after complete accretion contained 1–5 ocean masses of water (Jambon & Zimmermann, 1990; Hirschmann, 2006). A major depletion of hydrogen and other light elements by loss to space during later Earth history can be ruled out, because the expected depletions of light isotopes resulting from such a distillation process are not observed on the Earth.

Evidence on the present-day volatile content of the Earth's mantle comes from direct studies of mantle samples, particularly xenoliths, from measurements of water contents in basalts, which are partial melts formed in the shallow part of the upper mantle and from remote sensing by seismic methods and magnetotelluric studies of electrical conductivity. While the first two methods may provide constraints on all volatiles, remote sensing techniques are primarily sensitive to water (Karato 2006).

Pyroxenes in mantle xenoliths that were rapidly transported to the surface contain from <100 to about 1000 ppm of water (Skogby, 2006); olivines may be nearly anhydrous but sometimes contain up to 300 ppm of water (Beran &

Libowitzky, 2006). These observations show that the upper mantle is by no means completely dry (Bell & Rossman, 1992). However, estimating mantle abundances of water and other volatiles from such data is difficult, because samples often have lost water on their way to the surface; in some cases, this water loss is evident in diffusion profiles that may be used to constrain ascent rates (Demouchy *et al.*, 2006; Peslier & Luhr, 2006; Peslier *et al.*, 2008). Moreover, many of these xenoliths come from alkali basalts or kimberlites. The source region of these magmas may be more enriched in volatiles than the normal mantle.

Mid-ocean ridge basalts (MORB) tap a volatile-depleted reservoir that is believed to represent most of the upper mantle. Ocean island basalts (OIB) appear to come from a less depleted, likely deeper source. Probably the best constraints on volatile abundances in the mantle come from MORB and OIB samples that have been quenched to a glass by contact with sea water at the bottom of the ocean (e.g. Saal *et al.*, 2002; Dixon *et al.*, 2002); the fast quenching rate and the confining pressure probably suppressed volatile loss. In principle, one can calculate from observed volatile concentrations in quenched glasses the volatile content in the source, if the degree of melting and the mineral/melt partition coefficients of the volatiles are known. Such calculations, however, are subject to considerable uncertainties. A much more reliable and widely used method is based on the ratio of volatiles to certain incompatible trace elements, such as H_2O/Ce and CO_2/Nb (Saal *et al.*, 2002). These ratios are nearly constant in MORB glasses over a large range of H_2O and CO_2 contents that represent different degrees of melting and crystal fractionation. This means that the bulk mineral/melt partition coefficient of H_2O is similar to that of Ce and the bulk mineral/melt partition coefficient of CO_2 is similar to Nb. For equal bulk partition coefficients, the H_2O/Ce ratio and the CO_2/Nb ratio must be the same in the mantle source and in the basalt, independent of the degree of melting. Therefore, measured H_2O/Ce ratios and CO_2/Nb ratios of the basalts can be used together with the quite well-constrained Ce and Nb contents of the mantle to estimate the water and carbon dioxide content in the MORB and OIB sources. Using this method, Saal *et al.* (2002) estimated the volatile contents of the MORB-source upper mantle to be 142 ± 85 ppm H_2O (by weight), 72 ± 19 ppm CO_2, 146 ± 35 ppm S, 1 ± 0.5 ppm Cl and 250 ± 50 ppm F. In general, estimates of the water content in the depleted MORB source using similar methods yield values of 100–250 ppm by weight for H_2O. In particular, the work by Michael (1995) suggests some regional variability of the MORB source water content. Much higher volatile concentrations with up to about 1000 ppm of H_2O have been obtained for the OIB source region (e.g. Dixon *et al.*, 1997; Hauri, 2002). The CO_2 content in the OIB source may range from 120 to 1830 ppm CO_2 (Hirschmann & Dasgupta, 2009). If one assumes that the MORB source is representative for most of the mantle and the OIB source contributes a maximum of 40% to the total mantle, these numbers would translate to a total mantle carbon budget in the order of $(1–12) \cdot 10^{23}$ g of C (Dasgupta & Hirschmann, 2010). A similar calculation assuming 142 ppm H_2O in the MORB source and 1000 ppm H_2O in the OIB source would give a bulk water reservoir in the mantle of $2 \cdot 10^{24}$ g, i.e. about 1.4 ocean masses. The uncertainty in this estimate is, however, quite significant and the number given is likely to be only an upper limit of the actual water content.

Water has a strong effect on the physical properties, particularly density, seismic velocities and electrical conductivity of mantle minerals (Jacobsen, 2006; Karato, 2006). In addition, water may change the depth and the width of seismic discontinuities (e.g. Frost & Dolejs, 2007), because it stabilizes phases that can incorporate significant amounts of water as OH point defects in their structure. These effects may be used for a remote sensing of the water content in parts of the mantle that are not accessible to direct sampling. The dissolution of water as OH point defects in minerals generally reduces their density and both P and S wave seismic velocities (Jacobsen, 2006). This is mostly due to the formation of cation vacancies that usually – but not always

(e.g. Gavrilenko *et al.*, 2010) – is associated with the dissolution of water as OH point defects in silicates. As such, the effect of increasing water contents is qualitatively similar to the effect of increasing temperature. However, the ratio of P and S wave velocities v_p/v_s appears to be particularly sensitive to water as water in minerals affects S wave velocities much more than P wave velocities. The v_p/v_s ratio may therefore be able to distinguish the effects of water from temperature, although the effects may be subtle (Karato, 2011).

A property that is particularly sensitive to water is electrical conductivity, which may be greatly enhanced by proton conduction (Karato, 1990) (see also Chapter 5 of this book). Therefore, numerous studies on the effect of water on minerals such as wadslyeite and ringwoodite have recently been carried out, since these two main constituents of the Earth's transition zone are able to dissolve more than 2–3 wt % of water (Smyth, 1987; Kohlstedt *et al.*, 1996). Although there are some significant discrepancies between the available studies (Huang *et al.*, 2005; Yoshino *et al.*, 2008), it appears that a fully hydrated transition zone containing several wt % of water can be ruled out. The data may, however, be compatible with water concentrations up to 1000 or 2000 ppm by weight (Huang *et al.*, 2005; Dai & Karato, 2009b). Such concentrations, if confirmed, would imply that the transition zone is the most important reservoir of water in the mantle, containing roughly 0.5 ocean masses of water.

1.3 Water

1.3.1 Hydrous minerals in the mantle

According to available phase equilibria studies (e.g. Gasparik, 2003), the bulk of the Earth's mantle is made up by nominally anhydrous minerals, i.e. silicates and oxides that do not contain any H_2O or OH in their formula. Mantle xenoliths, however, while they mostly consist of olivine, pyroxenes, and garnet or spinel, sometimes do contain some hydrous minerals such as amphiboles or phlogopite-rich micas (Nixon, 1987), indicating that these phases may be stable in the mantle under some circumstances.

Experimental data on the stability range of hydrous mantle minerals (Frost, 2006) are compiled in Figure 1.1. At low temperatures and high pressures, a variety of dense hydrous magnesium silicates (DHMS) are stable, including phase A, D, E, and superhydrous phase B. However, Figure 1.1 also shows clearly that the stability range of these phases is far away from a normal mantle adiabat; they may perhaps exist in cold subducted slabs, but not in the normal mantle. Of all the DHMS phases, phase D with composition $MgSi_2O_4(OH)_2$ is stable at the highest pressures. A new aluminum-rich version of phase D has recently been described (Boffa-Ballaran *et al.*, 2010). All other hydrous phases shown in Figure 1.1 also contain some Na and/or K. Both alkali elements occur in normal mantle peridotite only at a minor or trace element level (typically about 0.3 wt % Na_2O and 0.03 wt % K_2O). The occurrence of these phases is therefore

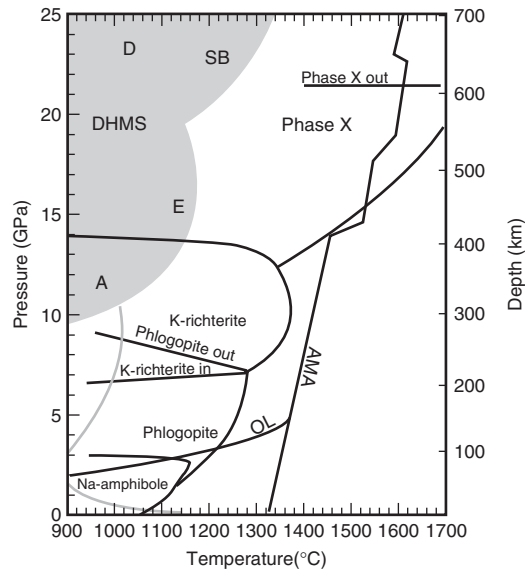

Fig. 1.1 Stability range of hydrous minerals in Earth's mantle. AMA is an average mantle adiabat, OL is a geotherm for a 100 million year old oceanic lithosphere. The thick black line gives the tentative location of the water-saturated peridotite solidus. Modified after Frost (2006).

not only limited by their maximum P,T stability field, but also by the availability of Na and K. At normal mantle abundances, most, if not all, Na and K may be dissolved in clinopyroxene (Harlow, 1997; Gasparik, 2003; Perchuk *et al.*, 2002; Harlow & Davies, 2004), so that these hydrous phases will not form, even in the pressure range where they may be stable for suitable bulk compositions. The only hydrous phase that is stable along an average mantle adiabat is phase X, a silicate with an unusual layer structure containing Si_2O_7 groups. The formula of phase X may be written as $(K, Na)_{2-x}(Mg, Al)_2Si_2O_7H_x$, where $x = 0–1$ (Yang *et al.*, 2001). The oceanic geotherm passes through the thermodynamic stability fields of phlogopite and Na-amphibole. The sodic amphiboles found in mantle samples are usually rich in pargasite $NaCa_2Mg_4Al_3Si_6O_{22}(OH)_2$ component, often with a significant content of Ti (kaersutites). However, due to the low abundance of alkalis in the normal mantle, their occurrence in mantle xenoliths is probably related to unusual chemical environments affected by subduction zone processes or mantle metasomatism. The same applies for phlogopite $KMg_3(OH)_2AlSi_3O_{10}$.

Hydrous phases are stable in some parts of subduction zones. The subducted slab contains hydrous minerals in the sediment layer. In addition, the basaltic layer and parts of the underlying peridotite may have been hydrated by contact with seawater to some degree. Anomalies in heat flow near mid-ocean ridges suggest that the uppermost 2–5 km may be hydrated (Fehn *et al.*, 1983). However, much deeper hydration may occur by the development of permeable fractures related to the bending of the slab when it enters the subduction zone (Faccenda *et al.*, 2009). For a long time, it was believed that amphibole in the basaltic layer is the major carrier of water into the mantle and that the volcanic front in island arcs is located above the zone of amphibole decomposition. More recent work (Poli & Schmidt, 1995; Schmidt & Poli, 1998), however, suggests that several phases in the sedimentary, basaltic and ultramafic parts of the slab are involved in transporting water, including amphibole, lawsonite, phengite and serpentine. Due to the formation of solid solutions in multicomponent systems, each phase decomposes over a range of pressures and temperatures, and the decomposition reactions of these phases overlap. Water released by decomposition of hydrous phases in the slab likely causes serpentinization of the shallow and cool parts of the mantle wedge above the slab. Under some circumstances, particularly for the subduction of old oceanic lithosphere along a cool geotherm, some of the serpentine in the ultramafic part of the subducted lithosphere may escape decomposition and may be able to transport water into the deep mantle (Rüpke *et al.*, 2004).

1.3.2 Water in nominally anhydrous minerals

Already more than 50 years ago, it was noticed that chemical analyses of nominally anhydrous minerals occasionally suggest the presence of traces of water (Brunner *et al.*, 1961; Griggs & Blacic, 1965; Wilkins & Sabine, 1973; Martin & Donnay, 1972). However, since water is an ubiquitous contaminant that may occur as mechanical impurities in samples, the significance of these observations was uncertain. This has changed by the application of infrared spectroscopy to the study of water in nominally anhydrous minerals, a method that was pioneered by the groups of Josef Zemann and Anton Beran in Vienna and by George Rossman at Caltech (e.g. Beran, 1976; Beran & Zemann, 1986; Bell & Rossman, 1992). Figure 1.2 shows polarized infrared spectra of an olivine crystal from the upper mantle. All of the absorption bands in the range between 3000 to 3700 cm^{-1} in such spectra correspond to OH groups (or, very rarely in a few minerals, to molecular H_2O). The intensity of absorption obviously depends on the polarization, i.e. on the orientation of the electrical field vector of polarized light relative to the crystal structure. This demonstrates that these samples contain ''water'' in the form of OH defects incorporated into the crystal lattice. If the bands were due to some mechanical impurities, a dependence of infrared absorption on the orientation of the crystal lattice would not be expected.

Infrared spectra are exceedingly sensitive to traces of water in minerals and can detect OH

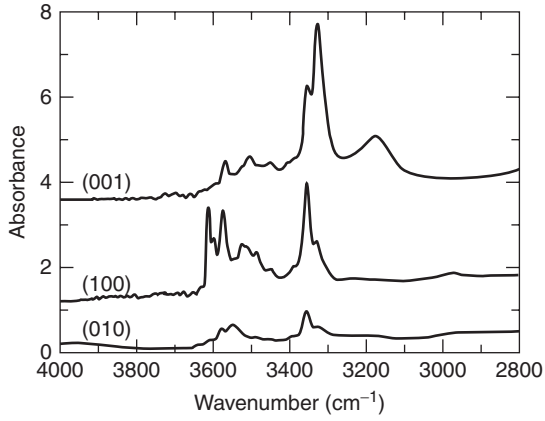

Fig. 1.2 Polarized infrared spectra of a water-containing olivine. The figure shows three spectra measured with the electrical field vector parallel to the a, b, and c axis of the crystal. Spectra courtesy of Xiaozhi Yang.

concentrations down to the ppb level, if sufficiently large single crystals are available. In principle, quantitative water contents can also be measured using the Lambert Beer law

$$E = \log I_0/I = \varepsilon \ c \ d, \qquad (1.1)$$

where E is extinction or absorbance, I_0 is infrared intensity before the sample, I is infrared intensity after the sample, ε is the extinction coefficient, c is concentration (of water) and d is sample thickness. Therefore, if the extinction coefficient of water in a mineral is known, water contents down to the ppb level can be accurately determined by a simple infrared measurement. Unfortunately, ε varies by orders of magnitude from mineral to mineral and ε may even be different for the same mineral, if OH groups are incorporated on different sites or by a different substitution mechanism, which results in a different type of infrared spectrum. Extinction coefficients therefore have to be calibrated for individual minerals by comparison with an independent and absolute measure of water concentration, such as water extraction combined with hydrogen manometry or nuclear reaction analysis (Rossman, 2006). Approximate numbers for water contents may also be obtained using empirical correlations between extinction coefficients and OH stretching frequencies (Paterson, 1982; Libowitzky & Rossman, 1997). Only in recent years has secondary ion mass spectrometry (SIMS) been developed sufficiently to be used to routinely measure water contents in minerals down to the ppm level (e.g. Koga *et al.*, 2003; Mosenfelder *et al.*, 2011). Unlike infrared spectroscopy, however, SIMS measurements do not yield any information on water speciation and, as such, they cannot directly distinguish between OH groups in the crystal lattice and mechanical impurities, such as water on grain boundaries, dislocations or fluid inclusions.

The recognition that nearly all nominally anhydrous minerals from the upper mantle contain traces of water (e.g. Bell & Rossman, 1992; Miller *et al.*, 1987; Matsyuk & Langer, 2004) has stimulated experimental studies of water solubility in these minerals. The suggestion by Smyth (1987) that wadsleyite could be a major host of water in the transition zone of the mantle, capable of storing several ocean volumes of water has further stimulated this work and it is now generally accepted that most of the water in the mantle occurs as OH point defects in nominally anhydrous minerals. Hydrous minerals, fluids or water-bearing silicate melts only form under special circumstances and at specific locations in the mantle. While the absolute concentrations of water in mantle minerals are low, due to the very large mass of the Earth's mantle they constitute a water reservoir probably comparable in size to the oceans, with a potential storage capacity several times larger than the ocean mass. In other words, most parts of the upper mantle are undersaturated with water, so that the actual OH contents in minerals are far below their saturation level.

Water is dissolved in silicates by protonation of oxygen atoms, charge balanced by Mg^{2+} vacancies, Si^{4+} vacancies and by coupled substitutions, such as $Al^{3+} + H^{+}$ for Si^{4+} or $Al^{3+} + H^{+}$ for 2 Mg^{2+}. Evidence for these substitution mechanisms comes from infrared spectra and from experimental observations. For example, certain

bands in the spectrum of olivine are only seen at low Si activities that may favor the formation of Si^{4+} vacancies, while other bands are enhanced at low Mg^{2+} activities and may therefore be associated with Mg vacancies (Matveev *et al.*, 2001). The occurrence of Mg vacancies in hydrous olivine was directly confirmed by single crystal X-ray diffraction studies (Smyth *et al.*, 2006). As a general rule, when the protonation of oxygen atoms is associated with cation vacancies, the protons are not located on the vacant cation site. Rather, their location is controlled by hydrogen bonding interactions with neighboring oxygen atoms. In the hydrogarnet $(OH)_4$ defect which corresponds to a fully protonated SiO_4 tetrahedron with a vacant Si site, the protons are located on the outside of the tetrahedron above the O-O edges (Lager *et al.*, 2005). Rauch and Keppler (2002) demonstrated that certain OH bands in the infrared spectra of orthopyroxene only occur in the presence of Al and are therefore assigned to coupled substitutions of H^+ and Al^{3+}. Similar studies have now also been carried out for olivine and several bands have been identified that are related to various trivalent cations and also to titanoclinohumite-like point defects (Berry *et al.*, 2005; 2007). Table 1.2 compiles the main substitution mechanisms for water in nominally anhydrous mantle minerals.

Water solubility, i.e. the amount of water dissolved in a mineral in equilibrium with a fluid phase consisting of pure water, can be described by the equation (Keppler & Bolfan-Casanova, 2006):

$$c_{water} = A\ f_{H_2O}^{n}\ \exp\left(-\frac{\Delta H^{1bar} + \Delta V^{solid} P}{RT}\right), \quad (1.2)$$

where A is a constant which essentially contains the entropy of reaction and n is an exponent related to the dissolution mechanism of OH: $n = 0.5$ for isolated OH groups, $n = 1$ for OH pairs (or molecular water), $n = 2$ for the hydrogarnet defect. ΔH^{1bar} is the reaction enthalpy at 1 bar and ΔV^{solid} is the change in the volume of the solid phases upon incorporation of water. Experimentally derived parameters for Equation (1.2) applied to the water solubility in a variety of nominally anhydrous minerals are compiled in Table 1.3.

Table 1.2 Hydrogen-bearing defects in nominally anhydrous minerals.

Substitution mechanism	Mineral	Reference
	—— Isolated protons ——	
$H^+ + Al^{3+} \leftrightarrow 2\ Mg^{2+}$	orthopyroxene	Mierdel *et al.* (2007)
$H^+ + Al^{3+} \leftrightarrow Si^{4+}$	orthopyroxene	Rauch & Keppler (2002)
$(Fe^3, Cr^{3+}, Sc^{3+}, REE^{3+}) + H^+ \leftrightarrow 2\ Mg^{2+}$	olivine	Berry *et al.* (2007)
$H^+ + B^{3+} \leftrightarrow Al^{3+}$	B-rich olivine	Sykes *et al.* (1994)
$H^+ + Li^+ \leftrightarrow Mg^{2+}$	possibly in pyrope	Lu & Keppler (1997)
	——— Proton pairs ———	
$2\ H^+ \leftrightarrow Mg^{2+}$	olivine	Smyth *et al.* (2006)
	enstatite	Rauch & Keppler (2002)
	wadsleyite	Smyth (1987)
	ringwoodite	Smyth *et al.* (2003)
	possibly $MgSiO_3$ perovskite	Ross *et al.* (2003)
$2\ H^+ + Mg^{2+} \leftrightarrow Si^{4+}$	possibly ringwoodite	Kudoh *et al.* (2000)
$Ti^{4+} + 2\ H^+ \leftrightarrow Mg^{2+} + Si^{4+}$	olivine	Berry *et al.* (2005)
interstitial H_2O	feldspars	Johnson & Rossman (2004)
	—— Cluster of four protons ——	
$4\ H^+ \leftrightarrow Si^{4+}$	garnet	Lager *et al.* (2005)
	possibly in olivine	Matveev *et al.* (2001)

Table 1.3 Thermodynamic models for water solubility in minerals.

Mineral	A (ppm/bar^n)	n	ΔV^{solid} (cm^3/mol)	ΔH^{1bar} (kJ/mol)	Reference
Olivine	0.0066	1	10.6	–	Kohlstedt *et al*. (1996)
	0.0147[a]	1	10.2	–	Mosenfelder *et al*. (2006)
	0.54	1	10.0	50	Zhao *et al*. (2004)[b]
$MgSiO_3$ enstatite	0.0135	1	12.1	−4.56	Mierdel & Keppler (2004)
Aluminous enstatite[c]	0.042	0.5	11.3	−79.7	Mierdel *et al*. (2007)
Jadeite	7.144	0.5	8.02	–	Bromiley & Keppler (2004)
Cr-diopside[d]	2.15	0.5	7.43	–	Bromiley *et al*. (2004)
Pyrope	0.679	0.5	5.71	–	Lu & Keppler (1997)
Ferropericlase	0.0004	0.5	4.0	–	Bolfan-Casanova *et al*. (2002)

Notes

Tabulated parameters refer to Equation (1.2). Where no value for ΔH^{1bar} is given, the enthalpy term is missing because the temperature dependence of water solubility was not calibrated and the equations are strictly valid only at the temperatures they were calibrated.

[a] Recalculated from a value of A = 2.45 H/10^{6}Si/MPa which in the original publication is probably misprinted as A = 2.45 H/10^6 Si/GPa.

[b] The equation by Zhao *et al*. (2004) also includes a term exp (αx_{Fa}/RT), where a is 97 kJ/mol and x_{Fa} is the molar fraction of fayalite.

[c] This equation gives the water solubility couples to Al of an Al-saturated enstatite. In order to get the total water solubility in Al-saturated enstatite, the water solubility in pure $MgSiO_3$ according to Mierdel *et al*. (2007) has to be added.

[d] These data may reflect metastable equilibria.

Since water fugacity increases with pressure, one would normally expect that at higher pressures, more water is dissolved in minerals. However, the term ΔV^{solid} in Equation (1.2) is usually positive and therefore counteracts the effect of increasing water fugacity. For this reason, water solubility in minerals usually first increases with pressure, and then decreases again. Depending on the sign and magnitude of ΔH, water solubility may either increase or decrease with temperature.

The partition coefficient of water between two phases α and β can be described as the ratio of the water solubilities in the two phases (Keppler & Bolfan-Casanova, 2006):

$$D^{\alpha/\beta}_{water} = \frac{c^{\alpha}_{water}}{c^{\beta}_{water}} = \frac{A_{\alpha}}{A_{\beta}} \; f_{H_2O}^{n_{\alpha}-n_{\beta}} \times \exp\left(-\frac{\left(\Delta H^{1bar}_{\alpha} - \Delta H^{1bar}_{\beta}\right) + (\Delta V^{solid}_{\alpha} - \Delta V^{solid}_{\beta})P}{RT}\right). \quad (1.3)$$

An important consequence of Equation (1.3) is that the partition coefficient may depend on water fugacity at given P and T if the two exponents n for the two phases are not equal. In other words, in such a case the partition coefficient may vary with bulk water content (e.g. Dai & Karato, 2009a).

Water storage in the upper mantle is largely controlled by olivine and orthopyroxene. Water solubility in garnet appears to be relatively low (Lu & Keppler, 1997) and no trace of water has ever been detected in the $MgAl_2O_4$ spinel phase of the upper mantle. Clinopyroxenes from mantle xenoliths may contain twice more water than coexisting orthopyroxenes (Skogby, 2006), but the very low modal abundance of clinopyroxene implies that it is not a major repository of water in the mantle. Clinoyroxene (omphacite) may, however, be very important for recycling water deep into the lower mantle in subducting slabs; this idea is consistent with the observation that the highest water contents from xenolith samples are usually found in eclogitic omphacites (Skogby, 2006).

Water solubility in olivine has been extensively studied (Kohlstedt *et al*., 1996; Zhao *et al*., 2004;

Mosenfelder *et al.*, 2005; Withers *et al.*, 2011). While earlier studies (e.g. Kohlstedt *et al.*, 1996) calculated water contents from infrared spectra using the Paterson (1982) calibration, later work suggested that this calibration underestimates the water contents of olivine by about a factor of three (Bell *et al.*, 2003). If this factor is taken into account, there is very good mutual consistency between the available studies. Water solubility increases continuously with pressure; Mosenfelder *et al.* (2005) observed 6399 ppm H_2O by weight at 12 GPa and 1100 °C. In addition, water solubility also increases with temperature (Zhao *et al.*, 2004; Smyth *et al.*, 2006), but at very high temperatures, observed water contents start to decrease again. This effect is likely related to a decrease of water activity in the coexisting fluid phase, not to an intrinsic reduction of water solubility in olivine. Smyth *et al.* (2006) found a maximum of 8900 ppm water in olivine at 12 GPa and 1250 °C.

Water solubility in orthopyroxene is very different from olivine. This is because in orthopyroxene, water solubility mostly involves coupled substitutions with Al^{3+}, such as Al^{3+} and H^+ replacing Si^{4+} or $Al^{3+} + H^+$ replacing 2 Mg^{2+}. Water solubility in pure $MgSiO_3$ enstatite is relatively low (Mierdel & Keppler, 2004), but increases greatly with Al (Rauch & Keppler, 2002; Mierdel *et al.*, 2007). If orthopyroxene coexists with olivine and an Al-rich phase such as spinel or garnet, the Al-content of the orthopyroxene is buffered. The water solubility in such an Al-saturated orthopyroxene decreases strongly with both pressure and temperature. This is probably partially due to the fact that the substitution of the larger Al^{3+} cation on the Si^{4+} site becomes unfavorable at high pressure. The contrasting behavior of water solubility in olivine and in orthopyroxene produces a pronounced minimum in water solubility in the upper mantle, which coincides with the depth of the seismic low velocity zone (Figure 1.3). The minimum in water solubility implies that water partitions more strongly into melts and therefore likely stabilizes a small fraction of partial melt in the seismic low velocity layer (Mierdel *et al.*, 2007).

At transition zone and lower mantle pressures, water solubility in minerals is not always easy to define, because the minerals usually coexist with a very solute-rich fluid or with a hydrous

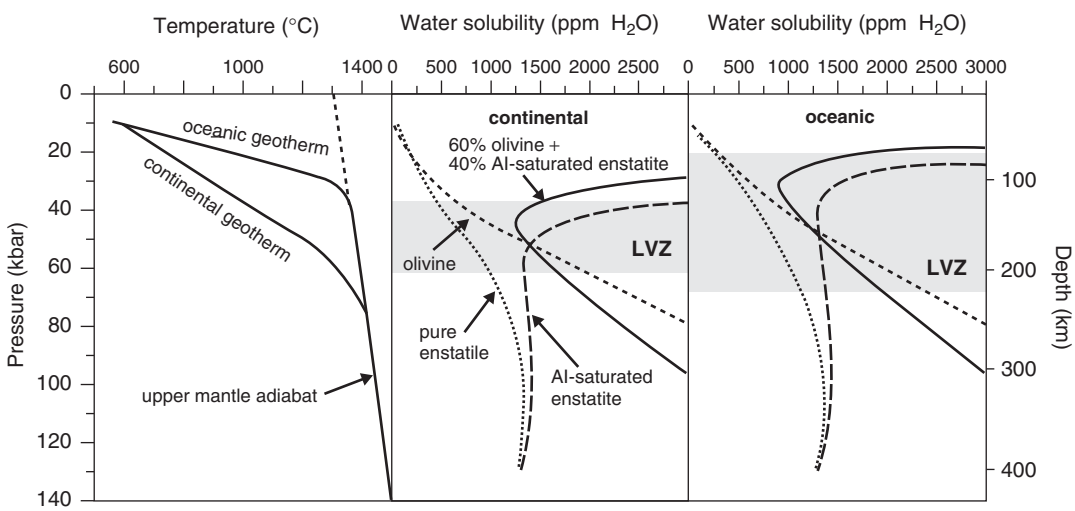

Fig. 1.3 Water solubility in the upper mantle as a function of depth, for an oceanic and a continental geotherm. LVZ = seismic low-velocity zone. Modified after Mierdel *et al.* (2007). Reprinted with permission from AAAS.

silicate melt of unknown water activity. This is because in the deep mantle, silicate melts and aqueous fluids are completely miscible, so that the composition of a fluid phase coexisting with minerals changes continuously from fluid-like to melt-like as a function of temperature (e.g. Shen & Keppler, 1997; Bureau & Keppler, 1999; Kessel *et al.*, 2005). Only in situations where water activity is buffered by phase equilibria (e.g. Demouchy *et al.*, 2005) a thorough thermodynamic treatment of the data is possible. In the deep mantle, the behavior of water is therefore often best described by the partition coefficient of water between solid phases and melts.

In the transition zone, most water is stored in wadsleyite and ringwoodite, the two high-pressure polymorphs of olivine. Compared to these two phases, majorite-rich garnet appears to dissolve less water (Bolfan-Casanova *et al.*, 2000). The prediction by Smyth (1987) that wadsleyite should be able to dissolve up to 3.3 wt % of water was confirmed by later experimental work (Inoue *et al.*, 1995: 3.1 wt % H_2O measured by SIMS; Kohlstedt *et al.*, 1996: 2.4 wt % measured by FTIR). Polarized infrared spectra (Jacobsen *et al.*, 2005) are consistent with the protonation of the electrostatically underbonded O1 site, as originally proposed by Smyth (1987). In contrast to wadsleyite, the observation by Kohlstedt *et al.* (1996) that spinel-structure $(Mg, Fe)_2SiO_4$ ringwoodite also dissolves up to 2.6 wt % of H_2O was unexpected, in particular considering that aluminate spinel appears not to dissolve any water. The dissolution of water in ringwoodite may be related to Mg vacancies and/or to partial disordering between Mg^{2+} and Si^{4+}, with some Mg^{2+} substituting for Si^{4+} and charge compensation by two protons (Smyth *et al.*, 2003; Kudoh *et al.*, 2000). Several studies have shown that the solubility of water in both wadsleyite and ringwoodite decreases with temperature above approximately 1300 °C, presumably due to reduced water activity in the coexisting melt phase. Litasov *et al.* (2011) estimate that the maximum water solubility in wadsleyite along an average mantle geotherm is about 0.4 wt %. The pressure effect on water solubility in both phases appears to be small. In equilibrium between wadsleyite and ringwoodite, water usually appears to partition preferentially into wadsleyite with $D^{wadsleyite/ringwoodite}$ of approximately 2 at 1450 °C; however, this partition coefficient may decrease with temperature (Demouchy *et al.*, 2005). Chen *et al.* (2002) report a partition coefficient $D^{wadsleyite/olivine} = 5$ for directly coexisting phases, which is roughly in agreement with predictions from solubility data. Deon *et al.* (2011) measured $D^{wadsleyite/olivine} = 3.7$ and $D^{wadsleyite/ringwoodite} = 2.5$. Similar data were reported by Inoue *et al.* (2010) and by Litasov *et al.* (2011).

The two main phases of the lower mantle, ferropericlase (Mg, Fe)O and $MgSiO_3$ perovskite appear to dissolve very little water, suggesting that the lower mantle may be largely dry (Bolfan-Casanova, 2005). The solubility of water in ferropericlase was systematically studied by Bolfan Casanova *et al.* (2002). A maximum water solubility of about 20 ppm H_2O by weight was observed at 25 GPa, 1200 °C and Re–ReO_2 buffer conditions.

Both the work by Bolfan-Casanova *et al.* (2000) and by Litasov *et al.* (2003) suggest that pure $MgSiO_3$ perovskite dissolves very little water, with maximum water solubilities in the order of a few or at most a few tens of ppm. Bolfan-Casanova *et al.* (2003) observed hydrous $(Mg, Fe)_2SiO_4$ ringwoodite to coexist with nearly dry $(Mg, Fe)SiO_3$ perovskite, yielding a water partition coefficient $D^{ringwodite/perovskite} = 1050$.

There is some controversy surrounding water solubility in Al-bearing $MgSiO_3$ perovskite. Murakami *et al.* (2002) reported about 0.2 wt % of water in magnesiumsilicate perovskite and 0.4 wt % water in amorphized calcium silicate perovskite synthesized from a natural peridotite composition at 25 GPa and 1600–1650 °C. Litasov *et al.* (2003) found up to 1400 ppm H_2O in perovskites containing up to 7.2 wt % Al_2O_3, with the water content increasing with Al. However, in all these studies, the infrared spectra of the perovskites show one very broad band centered near 3400 cm^{-1}, sometimes with some superimposed

weak and sharp peaks. A number of observations suggests that the broad band, which accounts for most of the water found in aluminous perovskites, is due to some mechanical impurities (i.e. inclusions of hydrous phases) and that the true water solubility in aluminous perovskites is very low. In particular, Bolfan-Casanova *et al.* (2003) showed that the broad infrared absorption band is only observed in perovskite samples that appear milky under the microscope. These samples also show Raman bands of superhydrous phase B and the infrared peaks of this phase coincide with the main infrared bands reported for aluminous perovskite. If only perfectly clear parts of aluminous perovskite are analyzed by infrared spectroscopy, observed water contents are very low and comparable to those observed for pure $MgSiO_3$ perovskite.

1.3.3 Water in silicate melts

Water is highly soluble in silicate melts and the associated melting point depression is essential for melting in subduction zones and at other locations in crust and mantle (e.g. Tuttle & Bowen, 1958; Kushiro, 1972). Water solubility increases with pressure and at low pressures, the solubility of often proportion to the square root of water fugacity (McMillan, 1994). There are subtle differences in water solubility between felsic and basic melts and even for felsic melts (e.g. Dixon *et al.*, 1995; Holtz *et al.*, 1995; Shishkina *et al.*, 2010), parameters such as the Na/K ratio can affect water solubility (Figure 1.4). In general, however, the solubility at given pressure and temperature is broadly similar for a wide range of melt compositions. Water solubility in melts can be measured with high precision, if melts can be quenched to bubble-free glasses, which may be analyzed by a variety of methods, including Karl-Fischer titration, infrared spectroscopy or SIMS (e.g. Behrens, 1995). However, for ultrabasic melts, for basic melts with high water contents and for any water-saturated melt beyond about 1 GPa, quenching to a homogeneous glass is usually not possible any more. Accordingly, while water solubility under subvolcanic conditions in the crust is very well known, it is only poorly constrained for melts in the deep mantle.

Because of the square root dependence of water solubility on water fugacity, it was believed

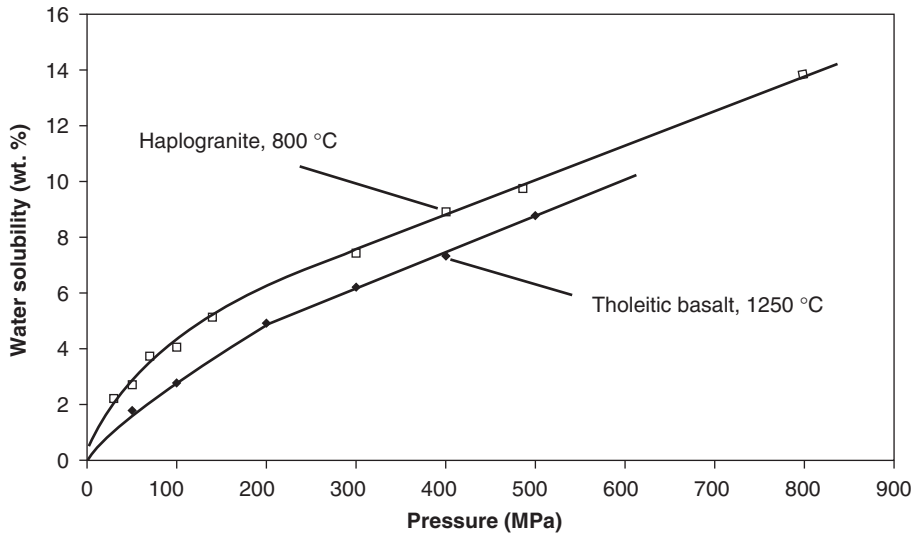

Fig. 1.4 Water solubility in haplogranitic melt at 800 °C (Holtz *et al.*, 1995) and in tholeitic basalt at 1250 °C (Shishkina *et al.*, 2010).

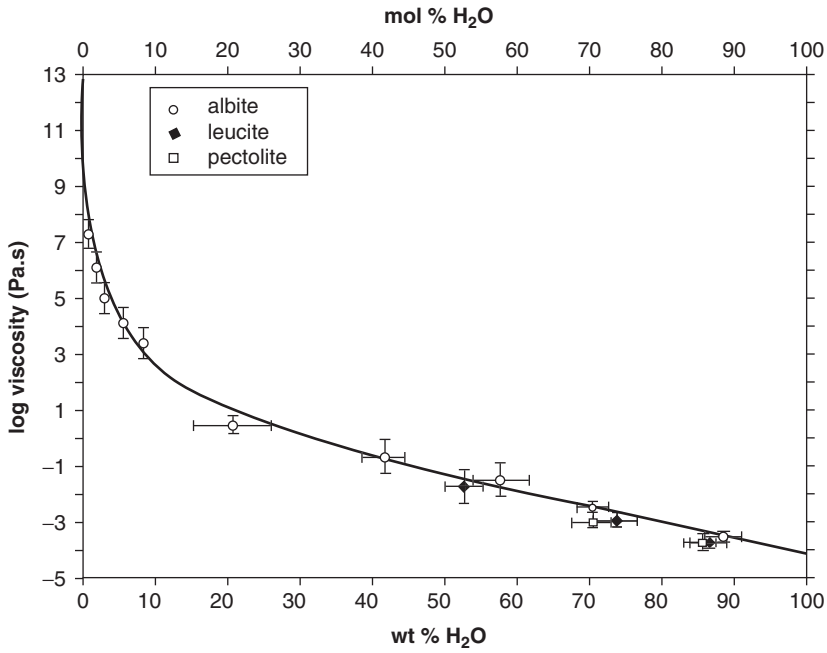

Fig. 1.5 Viscosity in the albite – H_2O system at 800 °C and 1–2 GPa. Modified after Audetat and Keppler (2004). Reprinted with permission from AAAS.

that water dissolves in silicate melts primarily as OH groups (e.g. Burnham, 1975), according to the reaction:

$$O^{melt} + H_2O^{gas} = 2\ OH^{melt}, \qquad (1.4)$$

where "O" is some oxygen atom in the anhydrous melt. Since even very small concentrations of water reduce the viscosity of silicate melts by orders of magnitude (Figure 1.5), a commonly held view is that water "depolymerizes" silicate melts by reacting with bridging oxygen atoms that connect two neighboring SiO_4 or AlO_4 tetrahedra, schematically:

$$H_2O + Si{-}O{-}Si = Si{-}OH + HO{-}Si. \qquad (1.5)$$

The simple model of water dissolution outlined above was modified when near infrared spectroscopy showed that quenched hydrous silicate glasses – and by inference, also the corresponding silicate melts – contain physically dissolved H_2O molecules in addition to OH groups (Bartholomew *et al.*, 1980; Stolper, 1982). Water speciation in silicate melts may therefore be described by the following equilibrium (as Equation (1.4):

$$O^{melt} + H_2O^{melt} = 2\ OH^{melt},$$

where O^{melt} is some bridging oxygen atom in the silicate melt. The equilibrium constant K_{wm} of this reaction

$$K_{wm} = \frac{a_{OH}^2}{a_O a_{H_2O}}, \qquad (1.6)$$

where a are activities, implies that the concentration of molecular water should increase with the square of the OH concentration. This means that molecular H_2O becomes abundant in the glass only at high water concentrations, while at low bulk water content, water is essentially dissolved only as OH groups. This is entirely consistent with the observed square root dependence of water solubility on water fugacity for low water contents. However, water speciation in glasses is only "frozen in" at the glass

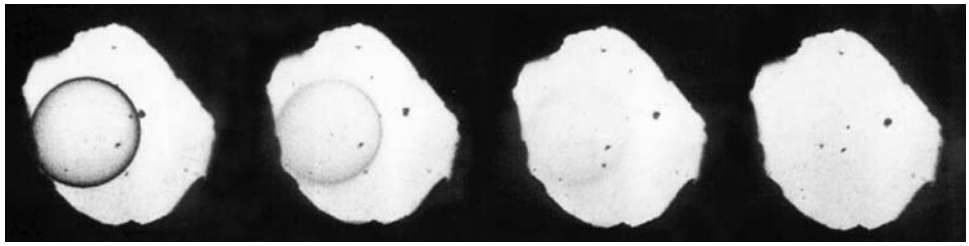

Fig. 1.6 Complete miscibility in the albite-H_2O system, as seen in an externally heated diamond anvil cell at 1.45 GPa and 763–766 °C. The optical contrast between a droplet of hydrous albite melt and the surrounding fluid disappears as the compositions of the coexisting phases approach each other. After Shen & Keppler (1997). Reproduced with permission of Nature.

transformation temperature, which may be very low for these water-rich systems. To obtain equilibrium constants for reaction (1.4), direct infrared spectroscopic measurements by water speciation at magmatic temperatures are necessary. Such measurements were first carried out by Nowak and Behrens (1995) and by Shen and Keppler (1995). They show that equilibrium (1.4) shifts to the right side with increasing temperature, so that at typical magmatic temperatures of 1000 °C or higher, OH groups dominate in the melts even if they contain several wt % of water. At pressures approaching 100 GPa, hydrogen becomes bonded to several oxygen atoms and forms extended structures in hydrous silicate melts (Mookherjee *et al.*, 2008).

The commonly held view that water depolymerizes silicate melts and glasses was challenged by Kohn *et al.* (1989) on the basis of NMR studies of hydrous albite glasses that failed to detect clear signs of depolymerization. The work by Kohn *et al.* has fostered intense research in the structural role of water in silicate melts and glasses. However, several more recent studies (e.g. Kümmerlen *et al.*, 1992; Malfait & Xue, 2010), often using more sophisticated NMR methods, appear to fully confirm the traditional view that water depolymerizes the structure of silicate melts and glasses by forming Si–OH and Al–OH groups, as indicated by Equation (1.5). In aluminosilicate glasses, however, the effects of depolymerization are not easily detected due to complications arising from Al/Si disorder in the glass and melt structure.

Water speciation in silicate melts is essential for understanding the strong effect of water on the physical properties of silicate melts; water does not only reduce viscosities by many orders of magnitude (e.g. Hess & Dingwell, 1996; Audetat & Keppler, 2005), it also greatly enhances electrical conductivity (e.g. Gaillard, 2004; Ni *et al.*, 2011) and diffusivity (e.g. Nowak & Behrens, 1997). While the effect on viscosity is likely due to depolymerization, i.e. due to the formation of OH groups, molecular water appears to be the main diffusing hydrous species. Water also reduces the density of silicate melts, but this effect appears to be rather insensitive to speciation and can be described by one nearly constant partial molar volume of water (Richet & Polian, 1998; Bouhifd *et al.*, 2001).

Since water solubility in silicate melts increases with pressure and since at the same time, the solubility of silicates in aqueous fluids also increases, the miscibility gap between water and silicate melts may ultimately disappear. This effect was already considered by Niggli (1920). Kennedy *et al.* (1962) showed that in the system SiO_2–H_2O the compositions of water-saturated melt and coexisting fluid approach each other close to 1 GPa. The first direct observation of complete miscibility in a silicate-H_2O system was reported by Shen and Keppler (1997), see Figure 1.6.

If complete miscibility between melt and fluid occurs, a water-saturated solidus cannot be defined any more. At low pressures, melting in a binary silicate-H_2O system in the presence

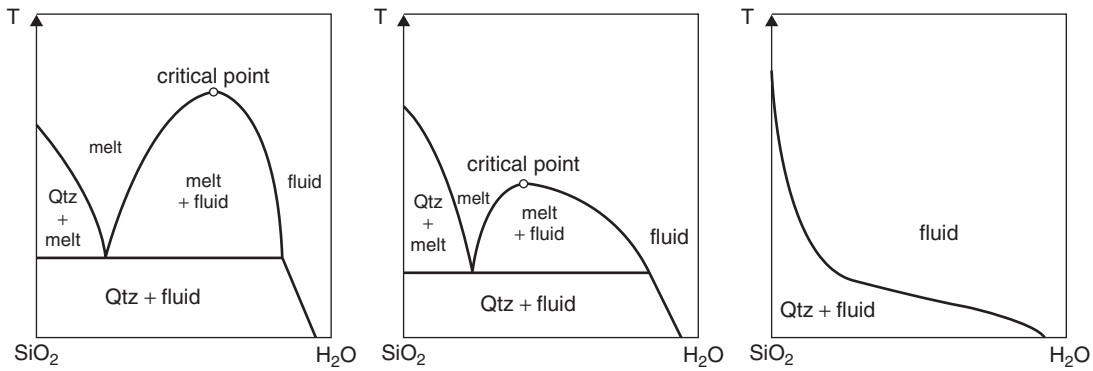

Fig. 1.7 Melting relationships in the SiO_2–H_2O system, schematic. Left: Melting below the critical curve; right: melting above the critical curve. After Keppler and Audetat (2005). Shown are the phase relationships for three different pressures, with pressure increasing from the left to the right diagram. Reprinted with permission from the European Mineralogical Union.

of an excess fluid phase occurs at a defined water-saturated solidus temperature, at which hydrous melt, fluid and solid silicate coexist. This is the situation on the left-hand side of Figure 1.7. A miscibility gap between the melt and the fluid allows both phases to coexist. However, with increasing pressure, the miscibility gap is getting smaller and finally disappears. In the absence of a miscibility gap (Figure 1.7, right diagram), a fluid of variable composition coexists with a solid at any temperature. The fluid composition is very water-rich at low temperature; with increasing temperature, the solubility of silicate in the fluid increases until it finally reaches the composition and properties of a hydrous silicate melt. Due to the continuous change from a ''fluid-like'' to a ''melt-like'' phase, the solidus temperature cannot be defined any more. In any binary silicate-H_2O system, a critical curve can be defined, which for a given pressure specifies the maximum temperature under which a melt and a fluid phase may coexist. The intersection of this line with the water-saturated solidus curve gives a critical endpoint at which the solidus curve ceases. Beyond the pressure of this critical endpoint, a water-saturated solidus cannot be defined any more and melting phase relationships resemble the situation shown on the right-hand side of Figure 1.7. Bureau and Keppler (1999) have mapped out critical curves for several felsic compositions; they suggest that in these systems the water-saturated solidus terminates at about 1.5–2 GPa. However, the location of the critical endpoint in basic to ultrabasic systems is not yet well constrained; it may occur somewhere in the 4–6 GPa range (Mibe *et al.*, 2004; Kessel *et al.*, 2005).

1.3.4 Hydrous fluids

Hydrous fluids are important agents of mass transport in subduction zones (e.g. Manning, 2004) and they are responsible for the formation of many economically important hydrothermal ore deposits (Hedenquist & Lowenstern, 1994). The properties of water under typical subvolcanic hydrothermal conditions, e.g. at 0.1 0.2 GPa and at 700–800 °C are very different from the water known at ambient conditions (Eugster, 1986; Franck, 1987). Liquid water under standard conditions is an extremely good solvent for ionic species; salts such as NaCl are highly soluble in water and they are practically completely dissociated into Na^+ and Cl^- ions. Similarly, HCl dissolved in water is a very strong acid with nearly complete dissolution into (hydrated) protons and Cl^- anions. This is due to the high dielectric constant ($e = 80$) of water under standard conditions. According to the Coulomb law, the attractive force between a pair of cation and

anion is reduced proportional to 1/e; therefore, in a solvent with $e = 80$, the attractive force between the two ions is just about 1% of the force expected in vacuum. This effect is responsible for the strong dissociation and the associated high solubility of many ionic solutes in water. At an atomistic level, the high dielectric constant is related to the polar nature of the angular H_2O molecules, which forms oriented layers around ions in such a way that the preferred orientation of the water molecules shields the electrical fields. However, at 0.1–0.2 GPa and 700–800 °C, the density of water (Burnham *et al.*, 1969; Pitzer & Sterner, 1994) is reduced to 0.2–0.4 g/cm^3 so that much less water molecules per volume unit are available to shield electrical charges; moreover the high temperature counteracts the formation of oriented dipole layers. For this reason, the dielectric constant of water under these typical magmatic hydrothermal conditions in the crust is only about 5, which is similar to a chlorinated hydrocarbon under standard conditions. Accordingly, the solvent behavior of water changes dramatically. Salts, such as NaCl, are not fully dissociated any more; rather they are dissolved as ion pairs or as multiple ion clusters and immiscibility between a water-rich vapor and a salt-rich brine may occur (Quist & Marshall, 1968; Bodnar *et al.*, 1985; Brodholt, 1998). HCl is only weakly dissociated and only a weak acid under these conditions (Frantz & Marshall, 1984). Since ionic substances are primarily dissolved as ion pairs, solubilities of cations strongly depend on the availability of suitable counter ions that allow the formation of stable ion pairs. This is the reason why under magmatic-hydrothermal conditions, the solubility of ore metals, such as Cu or Au, very much depends on the availability of halogens as ligands. The fluid/silicate melt partition coefficients of Cu, for example, increases by orders of magnitude in the presence of a few wt % of NaCl or HCl in the fluid (Candela & Holland, 1984; Keppler & Wyllie, 1991).

When pressure increases by several GPa to typical upper mantle conditions, dielectric constants and ionic dissociation increase again, with profound changes in the behavior of fluids. The changes of fluid properties are best rationalized as a function of temperature and fluid density (Burnham *et al.*, 1969; Pitzer & Sterner, 1984), rather than of temperature and pressure. This implies that the most profound changes in fluid properties actually occur in the 0–1 GPa range, with more subtle changes at higher pressures.

SiO_2 is the most important solute in hydrous fluids of the upper mantle. The solubility of SiO_2 in water has been well calibrated in several studies (e.g. Manning, 1984). The solution mechanism was studied by in-situ Raman spectroscopy in a hydrothermal diamond anvil cell by Zotov and Keppler (2000; 2002). These data show that silica is initially dissolved as orthosilicic acid H_4SiO_4 at low concentrations, which then polymerizes first to pyrosilicic acid dimers $H_6Si_2O_7$ and then to higher polymers, as solubility increases with pressure. This increasing polymerization of silica in the fluid, together with the depolymerization of silicate melts by water, provides an atomistic explanation for the occurrence of complete miscibility in silicate-H_2O systems. Viscosities in such systems increase continuously with silicate concentration (Figure 1.5, above); however, most of the increase occurs on the very silicate-rich side of the system, so that fluids with moderately high silicate content still retain very low viscosities (Audetat & Keppler, 2005).

The composition of aqueous fluids coexisting with $MgSiO_3$ enstatite and Mg_2SiO_4 forsterite in the system $MgO–SiO_2$ changes profoundly with pressure; while at 1 GPa, the solute appears to be rich in SiO_2, the MgO/SiO_2 ratio of the fluid as well as bulk solute concentration strongly increase with pressure (Ryabchikov *et al.*, 1982; Stalder *et al.*, 2001; Mibe *et al.*, 2002).

High field strength elements (HFSE), i.e. elements that form cations with a high charge and relatively small ionic radius, such as Ti^{4+}, Zr^{4+}, Hf^{4+}, Nb^{5+}, and Ta^{5+}, are generally poorly soluble in water, even at upper mantle pressures (Manning, 2004; Audetat & Keppler, 2005). As an example, Figure 1.8 shows experimental data on the solubility of TiO_2 in water. In the presence of silicates and aluminosilicates solutes, the solubility of these elements increases, but it still